# LIGHTCODE: Light Analytical and Neural Codes for Channels with Feedback

Sravan Kumar Ankireddy<sup>1</sup>, Krishna Narayanan<sup>2</sup>, Hyeji Kim<sup>1</sup>

<sup>1</sup>University of Texas at Austin <sup>2</sup>Texas A&M University, College Station

Abstract— The design of reliable and efficient codes for channels with feedback remains a longstanding challenge in communication theory. While significant improvements have been achieved by leveraging deep learning techniques, neural codes often suffer from high computational costs, a lack of interpretability, and limited practicality in resource-constrained settings.

We focus on designing low-complexity coding schemes that are interpretable and more suitable for communication systems. We advance both analytical and neural codes. First, we demonstrate that POWERBLAST, an analytical coding scheme inspired by Schalkwijk-Kailath (SK) and Gallager-Nakibŏglu (GN) schemes, achieves notable reliability improvements over both SK and GN schemes, outperforming neural codes in high signal-to-noise ratio (SNR) regions. Next, to enhance reliability in low-SNR regions, we propose LIGHTCODE, a lightweight neural code that achieves state-of-the-art reliability while using a fraction of memory and compute compared to existing deep-learning-based codes. Finally, we systematically analyze the learned codes, establishing connections between LIGHTCODE and POWERBLAST, identifying components crucial for performance, and providing interpretation aided by linear regression analysis.

Index Terms—Channels with Feedback, Deep Learning, Channel Coding, Feedback Coding, Finite Block Length Coding

#### I. Introduction

Shannon introduced the concept of feedback channel in [1]. In a channel with feedback, the transmitter *cooperates* with the receiver to improve the probability of successful transmission by utilizing the *feedback* from the receiver. In [1], Shannon assumes a perfect *noiseless* feedback channel with *unit delay* and demonstrates that the availability of feedback at the transmitter does not change the capacity of the resultant forward channel for memoryless channels. Interestingly, while the capacity remains the same, significant improvements in terms of error exponents can be achieved with the help of feedback.

One of the seminal schemes in the noiseless feedback setting has been provided by Shalkwijk and Kailath in [2], [3] (SK) using a simple linear encoding scheme resulting in a doubly exponential error exponent for finite block lengths. In [4], a two-phase variant of the SK scheme, which we refer to as Gallager-Nakibŏglu (GN), was discussed that can lead to further exponential decay of the error, provided a sufficiently good SNR is available for the forward channel. The SK scheme has been enhanced in various ways. The

Modulo-SK scheme [5] and schemes by Chance-Love [6] and Mishra et al [7], extends the SK scheme for noisy feedback, while compressed error correction (CEC) [8] and accumulative iterative code (AIC) [9] focus on reducing channel use through continuous error vector compression, using noiseless feedback.

While guaranteeing impressive error exponents, SK and other analytical coding schemes have not been adapted to practical communication systems, as the improvement in performance does not justify the cost incurred in terms of high-numerical precision, increase in the amount of feedback, and large number of rounds of communication. Because of this, analytical feedback coding schemes in practice are limited to automatic repeat request (ARQ) and hybrid-ARQ (HARQ) retransmission schemes, where the receiver provides simple one-bit feedback to indicate success (acknowledgment/ACK) or failure (negative acknowledgment/NACK). Extending ARQ to multi-bit feedback is an interesting research topic; for example, compressed error hybrid ARQ (CE-HARQ) [10] and Griffin et al. [11] propose using full feedback from the receiver to iteratively improve the error vector at the receiver.

Recent advances in deep learning revived the interest in coding for channels with feedback by leveraging the expressive power [12] of deep neural networks. Several works proposed deep learning approaches to improve the performance of channel codes, ranging from augmenting analytical decoders with learnable parameters [13]-[16] to creating novel neural network architectures based neural encoders and decoders [17], [18] and improving the code design using sequential models [19], [20]. For channels with feedback, deep learning techniques were used to design new encoding and decoding schemes that take advantage of the high-capacity feedback channel. Deepcode [21] modeled both encoder and decoder functions as recurrent neural networks (RNNs) to process a bit stream in a sequential manner to directly minimize the end-toend transmission error over an AWGN channel. Several works further explored this idea of using learning-based approaches for modeling the encoding and decoding operations, which can be broadly classified into the RNN family of codes [22]-[24] and the transformer family of codes [25], [26], discussed in detail in Section V. The current state-of-the-art is generalized block attention feedback (GBAF) [26], which uses selfattention and transformer architecture to perform block coding.

While these state-of-the-art deep-learning-based feedback codes provide tremendous improvements in BLER performance, they also come with significant memory and computational costs that may not be supported by the next generation of communication transceivers that operate with limited onboard resources. Therefore, it is desirable to develop lightweight codes that use simple schemes while providing desirable performance. To accomplish a reduced complexity coding scheme, we explore two different directions in this work. First, we review and understand the existing analytical feedback coding schemes to identify the limitations and propose a new feedback coding scheme that provides non-trivial performance improvements over the existing schemes for channels with passive, noiseless feedback. Next, we propose a lightweight deep-learning-based feedback coding scheme that can greatly reduce the complexity compared to neural block-feedback coding schemes by limiting ourselves to a symbol-by-symbol scheme instead of block coding schemes.

Our main contributions are summarized as follows:

- We provide a comprehensive review of the existing analytical and deep-learning-based coding schemes for channels with feedback and identify the limitations of existing approaches (Section III and Section V).
- We propose POWERBLAST, an analytical coding scheme that noticeably improves the performance over Schalkwijk-Kailath and two-phase Gallager-Nakibŏglu schemes (Section IV) and exhibits reliability comparable to state-of-the-art deep-learning-based coding schemes in regions of high-SNR (Section VII).
- We propose LIGHTCODE, a lightweight neural coding scheme that achieves a performance superior to current state-of-the-art feedback coding schemes using 10× fewer parameters and computational complexity (Section VI, Section VII), while maintaining interpretability.
- We analyze the representations learned by the LIGHT-CODE encoder using linear regression and draw comparisons with POWERBLAST. We also demonstrate that the relation between encoded symbols and the feedback is highly non-linear in the final rounds, underscoring the need for deep-learning-based coding scheme (Section VIII).

# II. SYSTEM MODEL

We consider a feedback coding scheme with an AWGN forward channel and an AWGN feedback channel with noisy passive feedback. The goal is to transmit a message vector  $\mathbf{u} \in \{0,1\}^K$  of length K to the receiver using a total of D channel uses, resulting in an overall coding rate of  $R = {}^K/D$ . In this work, we consider symbol-by-symbol coding, where the entire block of K bits will be mapped to one symbol. Hence, the terms block and symbol can be used interchangeably. Based on this, the number of rounds of communication for a rate  ${}^K/D$  code is D.

In the first round, the transmitter encodes the message block  $\mathbf{u} \in \{0,1\}^K$  to a real-valued output  $x_1 \in \mathbb{R}$  and transmits using the forward AWGN channel as

$$x_1 = \phi(\mathbf{u}),\tag{1}$$

$$y_1 = x_1 + n_1, (2)$$

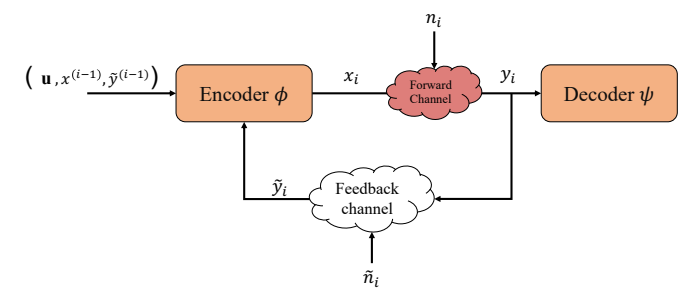


Fig. 1: Illustration of the  $i^{\rm th}$  round of communication for channels with feedback. The encoder takes as input the message bits  ${\bf u}$  and the encoder output from previous rounds  $x^{(i-1)}$ , concatenated with the feedback from previous rounds  $\tilde{y}^{(i-1)}$ , to compute  $x_i$ .

where  $n_1 \sim \mathcal{N}(0, \sigma_{ff}^2) \in \mathbb{R}$  denotes the feedforward noise. The receiver then sends the noisy received symbol as feedback using the feedback channel as

$$\tilde{y}_1 = y_1 + \tilde{n}_1,\tag{3}$$

where  $\tilde{n}_1 \sim \mathcal{N}(0, \sigma_{fb}^2) \in \mathbb{R}$  denotes the feedback noise.

At round i>1, the encoder  $\phi$  computes the output  $x_i$  using the input message bits  $\mathbf{u}$  and the encoder outputs from previous i-1 rounds  $x^{(i-1)}=\{x_1,\ldots,x_{i-1}\}$  and the feedback from previous i-1 rounds  $\tilde{y}^{(i-1)}=\{\tilde{y}_1,\ldots,\tilde{y}_{i-1}\}$  as

$$x_i = \phi(\mathbf{u}, x_1, \dots, x_{i-1}, \tilde{y}_1, \dots, \tilde{y}_{i-1}).$$
 (4)

At the end of D rounds of communication, the decoder  $\psi$  estimates the transmitted message vector  $\hat{\mathbf{u}}$  using the received symbols from all D rounds  $\{y_1, y_2, \dots, y_D\}$  as

$$\hat{\mathbf{u}} = \psi \left( y_1, y_2, \dots, y_D \right), \tag{5}$$

where  $\hat{\mathbf{u}} \in \{0,1\}^K$ . The objective is to design an encoder-decoder pair  $\{\phi,\psi\}$  that minimizes the probability of error  $\mathbb{P}\{\mathbf{u} \neq \hat{\mathbf{u}}\}$  for a given number of rounds D, under a sum power constraint of  $\sum_{i=1}^D \mathbb{E}[|x_i|^2] = D$ .

# III. ANALYTICAL CODING SCHEMES FOR CHANNELS WITH NOISELESS FEEDBACK

In this section, we review analytical coding schemes for channels with noiseless feedback i.e.,  $\sigma_{fb}^2 = 0$ . We begin by reviewing the celebrated Schalkwijk-Kailath coding scheme [2], one of the seminal works in coding for channels with noiseless feedback. We then proceed to review a less widely-known scheme by Gallager-Nakibŏglu [4]. This scheme is similar to the SK scheme for the first D-1 rounds. Still, it deviates greatly in the last round, tailoring for the transmission of discrete messages, often significantly improving the performance in one round of communication. The Gallager-Nakibŏglu (GN) scheme is typically not considered as a baseline as it exhibits a worse error rate compared to SK. However, in the next section, we introduce a novel analytical coding scheme, building on the SK and GN schemes. This new scheme achieves a significantly lower error rate than either the SK or GN schemes and is often comparable to highly complex neural coding schemes in high-SNR regions, defying the conventional belief that neural coding schemes are much more reliable than analytical ones.

# A. Schalkwijk-Kailath coding scheme

SK scheme considers the problem of transmitting a fixed number of bits on an AWGN forward channel and a noiseless feedback channel. The transmission begins by mapping K bits of information symbols to a single  $2^K$ -ary pulse-amplitude modulation (PAM) symbol  $\Theta$  from the constellation

$$\Theta \in \{\pm 1\eta, \pm 2\eta, \dots, \pm (2^K - 1)\eta\},$$
 (6)

where  $\eta = \sqrt{3/(2^{2K}-1)}$  is the scaling factor to ensure unit power normalization of the PAM constellation. We note that even though a block of information is transmitted since all the K bits of information are mapped to one PAM symbol, the SK scheme at its core can be considered a symbol-by-symbol feedback scheme. We now describe the SK coding scheme in detail.

In the first round, the uncoded PAM symbol is transmitted after accounting for power constraint P i.e.,  $x_1 = \sqrt{P}\Theta$  as

$$y_1 = x_1 + n_1, (7)$$

where  $n_1 \in \mathcal{N}(0,\sigma_{ff}^2)$  is the noise in the forward AWGN channel. The received symbol  $y_1$  is then sent back to the transmitter noiselessly. For the second round, the transmitter first computes the receiver's estimate of the transmitted symbol based on  $y_1$  as  $\hat{\Theta}_1 = \frac{y_1}{1+\sigma^2/P}$  using linear minimum mean square error (LMMSE) estimator. In the second round, after receiving  $y_1$  as feedback, the transmitter sends the scaled version of the *error* in the estimate from the previous round, i.e.,  $\epsilon_1 = \hat{\Theta}_1 - \Theta$ . This process continues for the remaining rounds. In other words, starting from round i=2, the goal of the transmitter is to transmit the error in estimate from the previous round,  $\epsilon_{i-1} = \hat{\Theta}_{i-1} - \Theta$ , after scaling appropriately to satisfy the power constraint. The complete algorithm is described in Alg. 1.

**Error analysis.** It is shown in [5] that the probability of error for rate K/D SK scheme is given by

$$p_{SK} = 2(1 - 2^{-K})Q\left(\sqrt{\frac{3S(1+S)^{D-1}}{2^{2K}-1}}\right),$$
 (8)

where S is the SNR of the forward AWGN channel on a linear scale.

# B. Gallager-Nakibŏglu coding scheme

In [4], Gallager-Nakibŏglu proposed a two-phase scheme that builds on the Elias scheme, which is also closely related to the SK scheme. While the SK scheme considers the problem of transmitting a discrete symbol, Elias [27] studied the problem of transmitting a Gaussian random variable  $U \in \mathcal{N}(0,\sigma^2)$ . The strategy for forward and feedback transmissions is similar to SK, where a scaled version of the error in the LMMSE estimate is transmitted in every round i>1. The main difference between the SK and Elias schemes lies in that the SK scheme aims to refine the message itself, while the Elias scheme aims to refine the noise added in the very first transmission.

GN scheme operates in two phases and relies on the assumption that after a sufficiently large number of rounds of

Algorithm 1: Schalkwijk-Kailath (SK) coding scheme

**Input:** Message symbol  $\Theta$ , number of rounds D, noise variance  $\sigma^2$ 

**Round 1: Tx:** Power normalization:  $x_1 = \sqrt{P}\Theta$ ;

Forward channel:  $y_1 = x_1 + n_1$ ;

Rx: LMMSE estimate of transmit symbol

 $\hat{\Theta}_1 = \frac{y_1}{1 + \sigma^2/P}$ ;

/\* Tx sends the error in estimate  $\hat{\Theta}_1 - \Theta$  over the next D-1 rounds \*/

while  $2 \le i \le D$  do

**Tx:** Compute the error in estimate of previous

round  $\epsilon_{i-1} = \hat{\Theta}_{i-1} - \Theta$ ;

Power normalization:  $x_i = \frac{\sqrt{P}}{\sigma_{i-1}} \epsilon_{i-1}$ , where

 $\sigma_{i-1}^2 = \mathbb{E}[\epsilon_{i-1}^2];$ 

Forward channel:  $y_i = x_i + n_i$ ;

**Rx:** LMMSE estimate of transmit symbol  $\sqrt{R}\sigma$ 

 $\hat{\epsilon}_{i-1} = \frac{\sqrt{P}\sigma_{i-1}}{P + \sigma^2} y_i ;$ 

Update the estimate of  $\Theta$  as:  $\hat{\Theta}_i = \hat{\Theta}_{i-1} - \hat{\epsilon}_{i-1}$ 

**Decoding:** Map  $\hat{\Theta}_D$  to the closest symbol in the  $2^K$  PAM constellation.

the Elias scheme, the effective SNR for the forward channel shall be adequately high for the noise variance to be considered small compared to the distance between the symbols in the PAM constellation. In such a high-SNR regime, a strategy superior to the Elias scheme can be implemented by taking advantage of the discrete nature of the signal. Instead of transmitting the original error vector with respect to  $2^K$ -ary PAM, the integer difference in the PAM index of the estimate and the true PAM symbol is transmitted. We refer to this as discrete-symbol scheme. This method results in an error exponent that decreases with an exponential order, which increases linearly with the number of rounds. For this work, we assume that the high-SNR region is realized in the final round of communication, which is valid according to the 2-phase strategy described in [4].

We now describe the GN scheme in detail. The first round of GN is simply uncoded PAM, except for the power allocation. In [4], it is shown the optimal power distribution across D rounds is attained by choosing  $P_1$  and  $P_2$  such that  $P_1 + (D-1)P_2 = DP$  and  $P_1 = P_2 + 1$  where  $P_1$  is the power constraint in round 1 and  $P_2$  is the power constraint in remaining rounds. Hence, the transmission in round 1 is given by

$$y_1 = \sqrt{P_1}\Theta + n_1. (9)$$

For the remaining rounds, the goal of the transmitter is to send the noise  $n_1$  to the receiver as in the Elias scheme, where the LMMSE estimate at the receiver is improved iteratively, and a maximum likelihood (ML) detection is used at the end of D-1 rounds of communication to map the estimate to the original PAM constellation.

Finally, for the last round, GN uses a discrete-symbol scheme suitable for the high-SNR region by transmitting the

error in the PAM index U. We follow the assumption from [4] that the high-SNR region guarantees that  $U \in \{-1, 0, 1\}$  with high probability. In [4], an ML decoder is used for the ease of analysis across multiple rounds of discrete symbol scheme, which is sub-optimal. However, since we are assuming only one round of the discrete-symbol scheme in this work, we assume a maximum-a-posteriori (MAP) decoder, which is optimal for the performance. Hence, the final round of GN can be viewed as MAP detection on a constellation  $\{-1, 0, 1\}$ with probability distribution  $\{p_{GN1}/2, 1-p_{GN1}, p_{GN1}/2\}$  where  $p_{GN1}$  is the probability of error after D-1 rounds. The complete algorithm is described in Alg. 4 in Appendix Section A.

**Error analysis.** The probability of error for a rate K/DGallager-Nakibŏglu scheme can be computed in two phases. The first phase can be analyzed as 1 round of uncoded PAM followed by D-2 rounds of Elias scheme, for which it is shown in [4] that the probability of error is given by

$$p_{GN1} = 2(1 - 2^{-K})Q\left(\sqrt{\frac{3(1 + S - \frac{1}{D-1})^{D-1}}{2^{2K} - 1}}\right),$$
 (10)

where S is the SNR of the forward AWGN channel on a linear scale.

In the final round, the discrete integer difference between the PAM index of the decoded message  $\hat{m}$  and the index of the true message m is transmitted, where  $(\hat{m} - m) \in \{-1, 0, 1\}$  with probability distribution  $\{p_{GN1}/2, 1 - p_{GN1}, p_{GN1}/2\}$  based on the assumption from [4]. The probability of error in decoding using a MAP decoder can thus be computed as

$$p_{GN} = 2(1 - p_{GN1})Q\left(\gamma\sqrt{S}\right) + p_{GN1}Q\left(\left(\frac{1}{p_{GN1}} - \gamma\right)\sqrt{S}\right),\tag{11}$$

where S is the SNR of the forward AWGN channel in linear scale and  $\gamma$  is the detection threshold given by

$$\gamma = \frac{1}{2\sqrt{p_{GN1}}} + \frac{\sqrt{p_{GN1}}}{S} \log \left( \frac{2(1 - p_{GN1})}{p_{GN1}} \right), \quad (12)$$

where S is the SNR of the forward AWGN channel in linear scale.

# IV. PROPOSED ANALYTICAL CODING SCHEME: **POWERBLAST**

In this section, we propose POWERBLAST, a hybrid 2phase scheme, to iteratively refine the LMMSE estimate of the PAM symbol at the receiver and shift to a discrete symbol scheme that takes advantage of the sparsity of the error in the estimate of the PAM index in the final round. Through theoretical analysis and empirical results, we demonstrate that the performance of POWERBLAST is better than both SK and GN, in several regimes of interest.

For a rate K/D code, POWERBLAST begins by mapping Kbits of information to a  $2^K$  PAM constellation and transmits the symbols on the forward AWGN channel. The receiver performs an LMMSE estimate and sends the estimate as feedback to the transmitter through the noiseless feedback channel. This continues for the first D-1 rounds. In the final round, POWERBLAST uses a discrete symbol strategy to send the error in the PAM index of the estimate. The complete algorithm is described in Alg. 2.

# **Algorithm 2:** POWERBLAST coding scheme

**Input:** Message symbol  $\Theta$ , number of rounds D, noise variance  $\sigma_{ff}^2$ 

**Round 1: Tx:** Power normalization:  $x_1 = \sqrt{P}\Theta$ ;

Forward channel:  $y_1 = x_1 + n_1$ ;

Rx: LMMSE estimate of transmit symbol

$$\hat{\Theta}_1 = \frac{y_1}{1 + \sigma_{ff}^2/P} ;$$

/\* Tx sends the error in estimate 
$$\hat{\Theta}_1 - \Theta$$
 over the next  $D-2$  rounds \*/

while  $2 \le i \le D - 1$  do

Tx: Compute the error in estimate of previous round  $\epsilon_{i-1} = \hat{\Theta}_{i-1} - \Theta$ ;

Power normalization:  $x_i = \frac{\sqrt{P}}{\sigma_{i-1}} \epsilon_{i-1}$ , where

$$\sigma_{i-1}^2 = \mathbb{E}[\epsilon_{i-1}^2]$$

$$\begin{split} \sigma_{i-1}^2 &= \mathbb{E}[\epsilon_{i-1}^2]; \\ \text{Forward channel: } y_i &= x_i + n_i; \end{split}$$

**Rx:** LMMSE estimate of transmit symbol

$$\hat{\epsilon}_i = \frac{\sqrt{P}\sigma_{i-1}}{P + \sigma_{ff}^2} y_i ;$$

Update the estimate of  $\Theta$  as:  $\hat{\Theta}_i = \hat{\Theta}_{i-1} - \hat{\epsilon}_{i-1}$ end

**Decoding after round** D-1: Map  $\hat{\Theta}_{D-1} = \frac{\hat{x_1}}{\sqrt{P_1}\eta}$  to the closest symbol in the  $2^K$  PAM constellation.

/\* High-SNR scheme for final round \*/

Round D: Tx: Compute the difference in PAM indices  $U = \hat{m} - m$ ;

Power normalization:  $x_D = \frac{\sqrt{P}U}{\sigma_{ff}};$  where  $U = \hat{m} - m;$ Transmit:  $y_D = x_D + n_D$ ;

Final Decoding: Use ML decoder to detect  $\hat{U}$  and detect original PAM signal using  $\hat{U}$ .

We note that POWERBLAST can be seen as a combination of SK and GN. The key difference between the SK scheme and the initial rounds of the GN scheme lies in the choice of information transmitted in the second round. In SK, the difference between  $\Theta$  and the LMMSE estimate  $\hat{\Theta}$  is transmitted, whereas in GN, the noise in the channel realization from round 1, n<sub>1</sub>, is transmitted. Hence, POWERBLAST can be interpreted as D-1 rounds of SK scheme followed by GN scheme for the final round, resulting in a non-negligible improvement in performance. The error analysis for the POWERBLAST scheme is provided below.

**Theorem 1** (Error Analysis). The probability of error for rate K/D POWERBLAST scheme is given by

$$p_{PB} = 2(1 - p_{SK})Q\left(\gamma\sqrt{S}\right) + p_{SK}Q\left(\left(\frac{1}{p_{SK}} - \gamma\right)\sqrt{S}\right)$$
(13)

where

$$p_{SK} = 2(1 - 2^{-K})Q\left(\sqrt{\frac{3S(1+S)^{D-2}}{2^{2K} - 1}}\right)$$
 (14)

and  $\gamma$  denotes the detection threshold and S denotes the SNR of the forward AWGN channel on a linear scale, and Q() is the standard Q-function.

*Proof.* We begin by computing the probability of error for phase 1, which consists of D-1 rounds of SK scheme. For ease of analysis, we follow the same assumption of [5], where the estimator after round one is assumed to be the minimum variance unbiased estimator instead of LMMSE implying,

$$\hat{\Theta}_1 = \frac{y_1}{\sqrt{P}}.\tag{15}$$

Further, based on Alg. 1, we can view the effective channel corresponding to rounds 1 to D-1 as one round with effective SNR  $S.1+S)^{D-2}$ , where  $S=P/\sigma_{ff}^2$  is SNR for the forward channel in linear scale. Further, it is straightforward to show that the probability of error incurred in transmitting a symbol from unit power normalized  $2^K$  PAM, using an optimal detector, is

$$p_e = 2(1 - 2^{-K})Q\left(\frac{\sqrt{P\eta}}{\sigma}\right)$$
$$= 2(1 - 2^{-K})Q\left(\sqrt{\frac{3S}{2^{2K} - 1}}\right),$$

where S is the forward channel SNR in linear scale and Q() is the Q-function. Hence, the effective probability of error after D-1 rounds of SK is

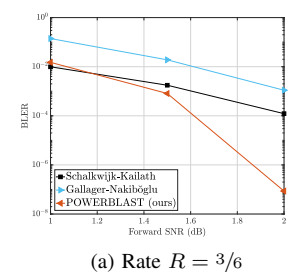
$$p_{SK} = 2(1 - 2^{-K})Q\left(\sqrt{\frac{3S(1+S)^{D-2}}{2^{2K} - 1}}\right).$$
 (16)

We now proceed to compute the probability of error for phase two, which is transmitting the difference in integer index over an AWGN channel. The key assumption for the high-SNR region is that the noise variance is small enough (compared to the effective forward SNR) that any errors beyond decoding to adjacent PAM symbols *i.e.*, errors beyond 1 index difference are essentially negligible [4]. Hence, the problem can be rephrased as finding the probability of error to communicate a symbol from the constellation  $\{-1,0,1\}$ , with probability distribution  $\{p_{SK}/2,1-p_{SK},p_{SK}/2\}$  using MAP decoder. This can be computed as

$$p_{PB} = 2(1 - p_{SK})Q\left(\gamma\sqrt{S}\right) + p_{SK}Q\left(\left(\frac{1}{p_{SK}} - \gamma\right)\sqrt{S}\right),\tag{17}$$

where  $\gamma$  is the detection threshold and S is the SNR of the forward AWGN channel on a linear scale.

**POWERBLAST vs. SK and GN schemes.** The performance comparison between the error expressions for a general SNR and rate is not straightforward (as they are represented in terms of Q functions). Instead, we limit our comparison to the canonical settings considered in the recent literature on channels with feedback (e.g., [26]), for rates  $^{3}/_{6}$  and  $^{3}/_{9}$  and plot the BLER performance in Fig. ??; we observe significant gains of POWERBLAST compared to both SK and GN in terms of the BLER performance.



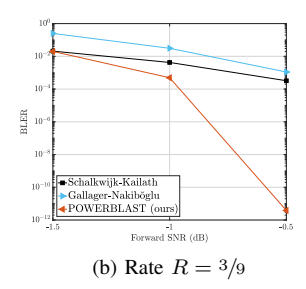


Fig. 2: By combining SK and discrete-symbol strategy of GN scheme, POWERBLAST noticeably improves the BLER performance upon both SK and GN schemes.

From the results so far, we have demonstrated that POWERBLAST provides the best performance among the analytically tractable solutions for channels with noiseless feedback that are recently considered in the literature (to demonstrate the reliability of deep-learning-based coding schemes [26]). In the coming sections, we consider deep-learning-based coding schemes such as GBAF and show that, surprisingly, the analytical POWERBLAST coding scheme often delivers competing performance. Nevertheless, POWERBLAST still falls short when the SNR is very low; thus, we investigate conditions under which deep-learning-based schemes provide the highest gain. Finally, we propose LIGHT-CODE, a lightweight neural coding scheme that achieves state-of-the-art performance with very low complexity.

# V. DEEP LEARNING BASED CODING SCHEMES

In this section, we review the current state of the learning-based codes for channels with feedback, closely analyze the generalized block attention feedback (GBAF) [26], discuss the shortcomings, and provide motivation for a new learning-based coding scheme we introduce in the next section.

# A. RNN families

deep-learning-based algorithms are capable of modeling complex input-output relations. One of the key challenges in designing codes for channels with feedback is accurately computing the next transmission that minimizes the probability of decoding error, conditioned on the feedback from previous rounds. Existing classical coding schemes employ linear estimators at the receivers and model the dependencies in a linear fashion at the transmitter, which is sub-optimal. Instead, the sequential nature of the feedback from previous can be better leveraged by using deep-learning architectures such as RNNs that are tailored for processing sequential data. Deepcode [21] demonstrated this advantage in modeling the dependencies across bits and rounds using bi-directional gated recurrent units (GRUs). Several follow-up works investigated the use of other RNN-based architectures such as long shortterm memory (LSTMs) [22], [23] and, more recently, Robust Coding [24] was proposed, which combined attention mechanism with bi-directional GRUs to optimize the symbol-bysymbol code design for noisy feedback channels across the rounds. Despite the promising performance, one disadvantage of using RNN-based architecture is the necessity to store the hidden states of the model, which are typically of much higher dimensions than the inputs and demand a lot of memory. Additionally, the sequential and iterative nature of encoding and decoding in RNNs can result in significant latency in the system.

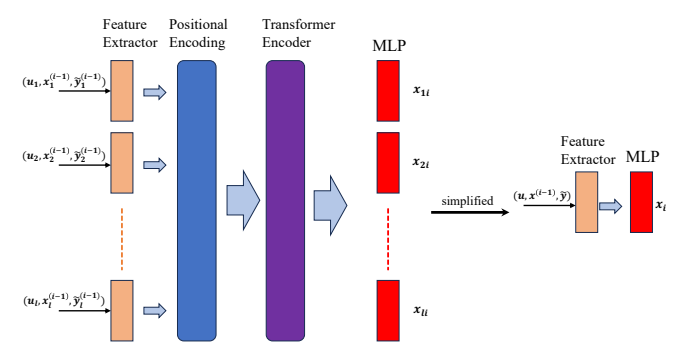


Fig. 3: (Left)Architecture for GBAF: The positional encoding and transformer encoding modules are used for block coding to encourage the mixing of symbols across the positions. (Right): Using a symbol-by-symbol scheme, LIGHTCODE significantly reduces the complexity of encoding and achieves more than 10x reduction in the number of parameters. On the left, we see the architecture for GBAF [26], and on the right, we see the architecture for LIGHTCODE (ours).

## B. Transformer families

In another line of work, self-attention-based transformer architectures have been explored for designing neural feedback codes. AttentionCode [25] introduced the idea of replacing RNN-based architecture with pure attention-based models, resulting in better alignment between a symbol and the corresponding feedback. More recently, GBAF [26] introduced the idea of performing block coding across the codeblock, in addition to coding across the rounds, resulting in orders of magnitude improvement in performance at extremely low SNRs.

As illustrated in Fig. 3, the encoding of GBAF is performed across the rounds by causally concatenating the message and feedback symbols from previous rounds and using a series of feature extractors and multi-layer perception (MLP) modules. Additionally, positional encoding (PE) and a self-attention-based transformer encoder layer are deployed to encourage the mixing of information across the symbols within a codeblock, leading to block coding. More specifically, a block of L bits is divided into l sub-blocks of K bits each and first encoded independently using a feature extractor. Next, PE and transformer encoder modules perform cross-symbol coding across the l symbols. Finally, an MLP module is used to encode each symbol. A similar architecture is used at the decoder.

For concreteness, in [26], GBAF considers a block size K=3 and codeblock length of L=51 and performs a block coding across l=17 symbols. This is the present state-of-the-art in performance, achieving a BLER of  $7\times 10^{-10}$  at SNR -1.0 dB for rate  $^3/9$ .

# C. Important open problems

While providing impressive performance in reliability, transformer architecture is computationally expensive. Further, it is well known that the transformer architecture does not scale well to larger sequences. The self-attention mechanism imposes a compute complexity of  $O(n^2)$  during training and O(n) during inference, even after using KV cache, with respect to input length n. Moreover, as the blocklength scales, a memory complexity of  $O(n^2)$  prohibits training the algorithm from using a large batch size, which is crucial for attaining a good performance for any deep-learning models.

An alternative approach would be to design a symbol-by-symbol coding scheme that can be scaled to any blocklength L by encoding K bits at a time independently. Within this context, an important question is: what is the extent of performance degradation compared to neural block coding schemes like GBAF? Moreover, it is necessary to formulate a novel and simplified architecture tailored to symbol-by-symbol processing. Finally, through streamlining the architecture and confining to symbol-by-symbol schemes, can we analyze and interpret the codes learned by deep learning models, discerning the reasons behind their notably superior performance compared to analytical counterparts?

In the coming sections, we answer all these questions. In Section VI, we systematically present LIGHTCODE, a lightweight symbol-by-symbol neural coding scheme, which achieves state-of-the-art BLER performance (Section VII). Further, we analyze GBAF to study the efficacy of block coding by performing a systematic ablation study and also analyze LIGHTCODE to identify the crucial components necessary for achieving ultra-low BLER in Section VIII.

# VI. PROPOSED NEURAL CODING SCHEME: LIGHTCODE

Our goal is to design lightweight neural codes without the need for block coding *i.e.*, we limit ourselves to symbol-by-symbol schemes suitable for both noiseless and noisy feedback settings. To this end, we design a lightweight deep-learning-based scheme with  $10\times$  fewer parameters compared to existing schemes. Surprisingly, this low-complex solution achieves a performance superior to current state-of-the-art deep-learning-based block-coding schemes. We now present the architecture and training choices that were crucial in achieving this new state-of-the-art BLER performance.

# *A.* LIGHTCODE: Architecture

Our architecture. We split the design of the encoder-decoder architecture into two parts: the feature extractor and the MLP module, as illustrated in Fig. 3 (right). The choice of the feature extractor plays a crucial role in determining the downstream performance. A higher complexity feature extractor can provide a better performance but might not be desirable for practical applications. For LIGHTCODE, after experimenting with various choices, we found that the design illustrated in Fig. 4 gave the optimal trade-off in complexity vs BLER performance. Specifically, we consider a hidden dimension of d=32 and 3 hidden layers. At the final layer, we use a skip connection to aggregate the outputs of layer 1

and layer 3 to project down to a latent dimension of d=16. The motivation for this architecture comes from our prior work on the design of deep-learning-based non-linear polar codes, DEEPPOLAR [18], where skip connections have proven to be crucial to ensure good performance. Finally, the output of the feature extractor will be passed to an MLP module to perform encoding or decoding. For the encoder, we choose a 2 layer MLP, and for the decoder, we choose a 1 layer MLP to transform the features into encoded representations or decoder outputs, respectively.

Our architecture vs. RNNs. A popular choice for modeling the cross-round relation in feedback coding has been the RNN family of architectures. The sequential nature of the data makes it suitable for RNNs, GRUs, LSTMs, and other similar architectures. While these architectures provided impressive performance, a significant drawback is the necessity to store the hidden states from previous encoding steps, which is a high-dimensional latent that requires a lot of memory. Hence, a feed-forward architecture, which does not need a hidden state, is a better choice for resource-constrained scenarios.

Our architecture vs. transformers. While transformer models overcome the issue of storing hidden states by using positional encoding and self-attention, they also come with great computational complexity. Moreover, recent transformer-based feedback coding schemes proposed block coding using self-attention, which requires  $O(n^2)$  memory with respect to codeblock length. Hence, a feed-forward architecture to perform a symbol-by-symbol coding scheme is more practical.

By carefully designing the architecture suitable for a symbol-by-symbol scheme, we achieve a lightweight design with more than  $10\times$  reduction in the number of parameters compared to the RNN family of schemes such as Robust Coding and transformer family of block coding schemes such as GBAF. Further, we show in Section VIII-C that this reduction in complexity provides up to  $171\times$  higher decoding throughput compared to Robust Coding and up to  $10\times$  higher throughput compared to GBAF. We now describe the encoding and decoding procedure in detail below.

**Encoding.** At round i, the encoder takes as input the original message and any available feedback from previous i-1 rounds to compute  $x_i$ . Further, after every round, a power reallocation is done across the rounds, similar to Deepcode [21]. This is also based on the theoretical justification that allocating more power to the initial rounds results in an optimal performance [4]. The resulting encoding process at round i is

$$x_i = \alpha_i \phi(\mathbf{u}, \tilde{y}_1, \tilde{y}_2, \dots, \tilde{y}_{i-1}), \tag{18}$$

where  $\tilde{y}_i = x_i + n_i + \tilde{n}_i$  is the feedback from the previous round and  $\alpha_i$  is the scaling factor to ensure sum power constraint across the rounds  $\sum_{i=1}^{D} \alpha_i^2 = D$ .

**Decoding.** At the end of D rounds of transmission, the decoder uses all the received symbols and estimates the original message  $\hat{\mathbf{u}}$  as

$$\hat{\mathbf{u}} = \psi(y_1, y_2, \dots, y_D),\tag{19}$$

where  $y_i = x_i + n_i$  is the noisy received symbol in round i.

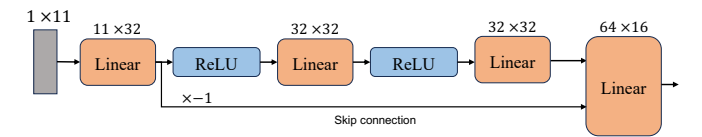


Fig. 4: Feature extractor design for LIGHTCODE.

Here,  $\phi$  and  $\psi$  are the encoder and decoder neural networks based on the architecture in Fig. 3. Using this simple symbol-by-symbol scheme, LIGHTCODE archives a performance similar to that of GBAF. It turns out that the computationally intensive self-attention mechanism and the cross-symbol coding are not adding considerable value to GBAF, as will be evidenced by our ablation studies in Section VIII-A.

**Choice of feature vectors.** Empirically, we observed that the choice of input to the feature extractor has a noticeable effect on the BLER performance based on the feedback channel. For noiseless feedback, the input features  $(\mathbf{u}, y_1, y_2, \ldots, y_i)$  worked the best. Further, as will be evident from discussions in Section VII-C, the input features  $(\mathbf{u}, x_1, x_2, \ldots, x_i, n_1 + \tilde{n}_1, n_2 + \tilde{n}_2, \ldots n_i + \tilde{n}_i)$  gave the best performance for noisy feedback. Apart from this difference, the rest of the architecture remains the same for noiseless and noisy feedback scenarios.

**Support for multiple rates.** One of the limitations of existing symbol-by-symbol coding schemes is the inability to serve a variety of rates *i.e.*, only rates of the form  $^1/D$ ,  $D \in \mathbb{Z}^+$  are supported. In order to overcome this, instead of processing 1 bit at a time, LIGHTCODE encodes a block of K bits into 1 symbol and communicates this symbol to the receiver over D rounds. By independently varying K and D any rate of the form K/D where,  $K, D \in \mathbb{Z}^+$  can be supported, making the scheme more flexible, while simultaneously reducing the overall latency of the communication by a factor of K. The results for multiple rates for a block length of K = 3 are discussed in Table II.

# B. Training

Our primary region of interest is rate  $^{3}/_{9}$  code at SNR -1.0dB, where our target BLER is  $\approx 10^{-9}$ . This is the current state-of-the-art performance by GBAF [26]. In order to achieve such an extremely low error rate, it is important to reliably train and simulate large amounts of samples. Inspired by the high-SNR variant of Gallager-Nakibŏglu [4], we hypothesize that in regions of high-SNR or low errors, a significant benefit to the forward transmission arises from the power reallocation to symbols with non-zero errors. This can only be realized during the training by considering a large batch and enforcing the power constraint per batch. Moreover, it is well understood that deep-learning models generalize better when trained with large batch sizes. Hence, we consider an extremely large batch size of  $10^5$ . While this is significantly larger compared to GBAF, which has a batch size of 8192, it is still a smaller number of symbols, considering that GBAF contains 17 symbols per codeblock, whereas our scheme consists of only 1 symbol per codeblock. Further, it is possible for us to train with such a large batch size because of the small number of parameters compared to other deep-learning-based coding schemes. For a fair comparison, we follow a training methodology similar to that of GBAF, as explained below.

# **Algorithm 3:** Training LIGHTCODE

**Input:** Encoder model  $\phi$ , Decoder model  $\psi$ , Block length K, number of rounds D, noise variance  $\sigma_{ff}^2$ , batch size B, number of epochs E, learning rate 1r

for  $i \le E$  do

Generate batch of random binary vectors 
$$\mathbf{u} \in \{0,1\}^{K \times B}$$

$$\begin{array}{l} \mbox{for } i \leq D \mbox{ do} \\ \\ x_i = \phi \left( \mathbf{u}, y_1, y_2, \ldots, y_{i-1} \right) \; ; \quad / * \mbox{ Encoding} \\ \mbox{at round } i \ * / \\ \\ y_i = x_i + n_i \end{array}$$

#### end

$$\mathbf{p_u} = \psi(y_1, y_2, \dots, y_D)$$
 ; /\* Decoding after  $D$  rounds \*/

Compute the NLL loss  $\frac{1}{B}\sum_{j=1}^{B}L_{\rm NLL}(\mathbf{c_j},\mathbf{p_{u_j}})$ , where  $\mathbf{c_j}$  is the class index corresponding to  $j^{\rm th}$  message vector  $\mathbf{u_j}$  and  $\mathbf{p_{u_j}}$  is class probability vector after the SoftMax layer.

Clip the gradients to 0.5.

Update model parameters for  $\phi$  and  $\psi$  using AdamW optimizer with learning rate lr.

Update the learning rate using LambdaLR.

end

We use AdamW optimizer, a stochastic optimization method that modifies the typical implementation of weight decay in Adam by decoupling weight decay from the gradient update. We initialize the learning to  $10^{-3}$  and use a LambdaLR scheduler with a weight decay of 0.01. Additionally, we clip all the gradient values to 0.5 for numerical stability. Starting with randomly initialized weights, we train the encoder and decoder models simultaneously on  $1.2 \times 10^5$  batches. Each input symbol corresponds to K bits, resulting in a  $2^K$  category classification problem for the decoder. Accordingly, we use cross entropy (CE) loss to measure the performance as

$$L_{\text{CE}} = \frac{1}{B} \sum_{i=1}^{B} \left( \sum_{j=0}^{2^{K}-1} c_{ij} \log p_{ij} \right),$$

where B is the batch size,  $2^K$  is the number of classes,  $c_{ij}$  is the true class probability and  $p_{ij}$  is the predicted probability of the  $j^{\text{th}}$  class, for the  $i^{\text{th}}$  sample.

The hyperparameters used for training the rate  $R=\mbox{$^3/\!\!9$}$  code are listed in Table I.

Once the training is complete, we compute the mean power and standard deviation for the encoded data after every round for a large number of samples,  $O(10^6)$ , to reliably estimate the

Hyperparameter	Value
Encoder training SNR	-1.0 dB
Decoder training SNR	-1.0 dB
Mini batch size $(B)$	100,000
Total epochs $(E)$	120
Batches per epoch	1000
Initial learning rate (lr)	$10^{-3}$
Optimizer	AdamW

TABLE I: Hyperparameters used in model training for rate <sup>3</sup>/<sub>9</sub>, SNR -1.0 LIGHTCODE.

mean and standard deviation corresponding to encoder outputs to be used during inference. This is crucial in enforcing the power constraint in expectation. The algorithm for training LIGHTCODE is described in detail in Algorithm 3.

# VII. MAIN RESULTS

We begin by comparing the performance of LIGHTCODE with the current state-of-the-art in deep-learning-based coding schemes for noiseless passive feedback setting, GBAF [26] and other schemes, demonstrated in Fig. 5. Next, we discuss a method for extending LIGHTCODE to moderate block-length regimes of up to L=300 and study the performance.

Finally, we look at deep-learning-based coding schemes for noisy feedback settings and how LIGHTCODE can be extended to this setting with minimal changes. We then proceed to compare the BLER performance for the same configuration as before but with a feedback SNR of 20 dB.

# A. LIGHTCODE and POWERBLAST vs. existing neural codes for noiseless feedback

In this section, we evaluate the performance of LIGHTCODE and POWERBLAST and compare them against several existing analytical and deep-learning feedback schemes. For concreteness, we consider the canonical setting of rate  $R=\sqrt[3]{9}$  with block length K=3 and a number of rounds D=9 transmitted on AWGN forward channel and noiseless feedback.

**Baselines.** Our primary comparison is against GBAF [26], which is the current state-of-the-art for the noiseless passive feedback setting. Additionally, we consider Deepcode [21], DEFC [22], DRFC [23], Attentioncode [25], and Robust Coding [21]. Additionally, for completeness as well as to understand the relative gains of deep-learning-based coding schemes, we also compare the performance against Schalkwijk-Kailath [2], Gallager-Nakibŏglu [4] and POWERBLAST.

In Fig. 5, we compare the BLER performance of rate  $^3/^9$  coding schemes. LIGHTCODE consistently outperforms the existing deep-learning-based schemes, including GBAF, while utilizing  $< ^1/_{10}$  the number of parameters. Moreover, these results indicate that POWERBLAST surpasses the performance of all existing schemes, including LIGHTCODE, when an adequately high signal-to-noise ratio is provided, which is -0.5 dB for rate  $^3/_9$ . However, at lower SNRs, the performance of deep-learning codes is significantly better.

**Multiple rates.** The coding rate of LIGHTCODE is determined by two factors, block length K and number of rounds of communication D. We now keep the block length constant

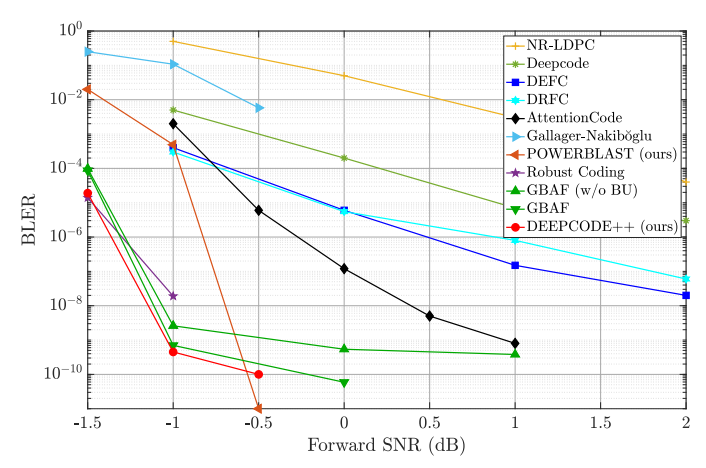


Fig. 5: Performance comparison of LIGHTCODE with GBAF and other existing neural feedback codes for rate  $^3/_9$  and noiseless feedback. LIGHTCODE achieves superior BLER performance compared to GBAF while utilizing  $<1/_{10}$ <sup>th</sup> the number of parameters.

and vary D to compare the performance against GBAF across multiple rates, as shown in Table II. LIGHTCODE consistently outperforms GBAF across a range of rates  $\{3/8, 3/7, 3/6, 3/5\}$ , while utilizing a fraction of the number of parameters.

SNR (dB)	Rate	GBAF	POWERBLAST	LIGHTCODE
-1.0	3/9	$7 \times 10^{-10}$	$2.8 \times 10^{-4}$	$4.5\times10^{-10}$
0.0	3/8	$6.1 \times 10^{-8}$	$8.8 \times 10^{-7}$	$5.1  imes 10^{-9}$
1.0	3/7	$7.5 \times 10^{-8}$	$1.0 \times 10^{-8}$	$1.0  imes 10^{-8}$
2.0	3/6	$1.5 \times 10^{-6}$	$1.5 \times 10^{-8}$	$8.3  imes 10^{-7}$
3.0	3/5	$8.7 \times 10^{-7}$	$1.9 \times 10^{-4}$	$2.7  imes \mathbf{10^{-7}}$

TABLE II: BLER performance comparison of LIGHTCODE with GBAF with POWERBLAST for different rates. LIGHTCODE consistently performs better than GBAF while using  $< 1/10^{th}$  the number of parameters.

# B. Performance in moderate blocklength regime

Using a code designed for K=3, it is straightforward to encode larger blocks of length L by treating the message as a packet of l=L/K independent symbols. Hence, the packet error rate (PER) for a packet of size l can be considered BLER for blocklength L. This modular approach to encoding is motivated by two key observations. The first is from the ablation studies in Section VIII-A, which demonstrate that explicit block coding is not beneficial in this regime and does not scale well. Second is the increase in computational complexity of both encoder and decoder modules associated with block coding. Results from Fig. 6 illustrate that LIGHTCODE scales gracefully with blocklength by independently encoding information in sets of K=3, keeping the complexity constant. Further, we also note that the bit error rate (BER) remains constant regardless of the blocklength L.

# C. Coding for Channels with Noisy Feedback

Finally, we now consider the case of channels with noisy feedback *i.e.*,  $\sigma_{fb}^2 > 0$ . While the assumption of noiseless feedback is easier to study, most practical feedback channels suffer from noise even when the receiver sending the feedback

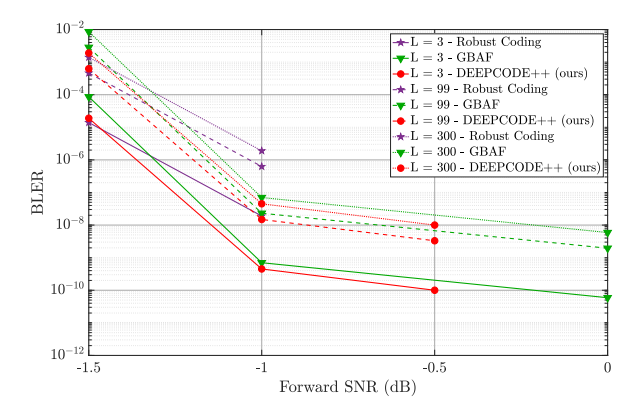


Fig. 6: deep-learning-based coding schemes scale gracefully with the length, providing a flexible way to code for any length without an increase in computational complexity.

operates at high power. Because of this limitation, both SK and GN schemes do not perform well. To address this, [6] introduces a linear feedback scheme that is implemented as an inner code to a concatenated code, which was found to be optimal within the linear family of codes [28]. More recently, [7] proposed using dynamic programming to improve the performance, which turns out to be a generalized version of SK. However, despite these improvements, the linearity of these schemes severely limits the performance that can be achieved.

Recalling the architecture of deep-learning-based schemes introduced in Section V, one of the interesting properties of these codes is their robustness to noise in the feedback channel. By taking advantage of the general architecture, it is straightforward to inject noise into the feedback channel during training to make the encoder-decoder robust. Hence, learning-based schemes can help design a practically realizable class of codes that can trained purely in a data-driven fashion and can provide gains under both noiseless and noisy feedback settings.

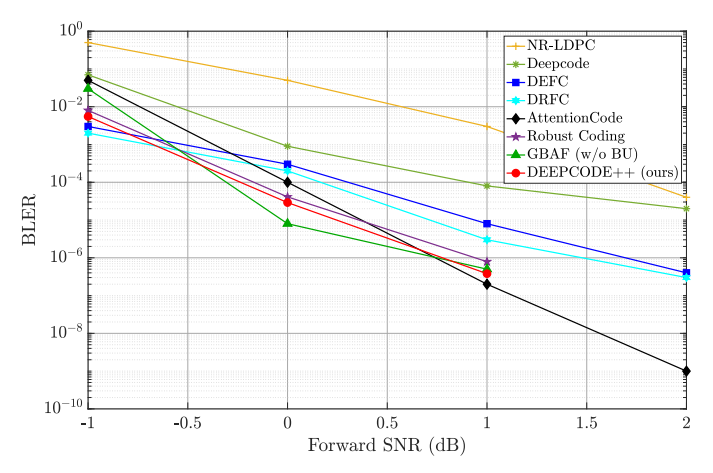


Fig. 7: Performance comparison of LIGHTCODE with GBAF and other existing neural feedback codes for rate  $^3/_9$  and noisy feedback with SNR = 20 dB. LIGHTCODE achieves BLER performance comparable to GBAF while utilizing only  $^1/_{10}$ th the number of parameters.

For training LIGHTCODE on noisy feedback channels, em-

pirically, we found that selecting the input features as the previous encoder outputs  $x_1$  and the cumulative noise  $n_i + \tilde{n}_i$  separately works better than directly passing the feedback  $\tilde{y}_i$  from previous rounds, which was the choice for noiseless feedback. Except for the change in input feature, the rest of the architecture and training details remain the same as the noiseless feedback setting. In Fig. 7, we compare the performance of rate  $^3/9$  LIGHTCODE against existing schemes, for a feedback SNR of 20 dB. We see that LIGHTCODE exhibits similar performance compared to GBAF while still utilizing only a fraction of the number of parameters.

## VIII. ANALYSIS

As evident from results in Section VII, symbol-by-symbol neural schemes can achieve performance comparable to block coding schemes such as GBAF. Consequently, we examine GBAF and LIGHTCODE in greater detail to systematically analyze their architecture, training process, and performance, with the aim of identifying the key factors contributing to their performance. Furthermore, we compare the memory and computational complexity of LIGHTCODE with existing schemes to quantify the gains. Finally, we provide an interpretation of the encoded representations of LIGHTCODE.

#### A. Ablation studies on GBAF

We investigate the contribution of the self-attention mechanism to the performance of GBAF by performing an ablation study to understand the compute vs performance trade-off better. First, the self-attention mechanism is disabled, and it is observed that this has no significant effect on the BLER performance. Next, both self-attention and positional encoding blocks are disabled, and the performance remains approximately the same. These results, provided in Table III, demonstrate a surprising observation that the self-attention and PE modules, which are responsible for cross-symbol block coding, contribute only marginally to the performance of GBAF. This brings into question the value of block encoding and motivates us to find simpler designs that perform only symbol-by-symbol coding while providing competing performance.

SNR (dB)	GBAF	GBAF (no attn)	GBAF (no attn, no PE)
-1.5	9.8e-5	7.5e-5	2.6e-5
-1.0	2.6e-9	1.2e-9	2.7e-9
0.0	5.4e-10	6.6e-10	8.1e-10

TABLE III: Effect of block coding on performance of GBAF for rate <sup>3</sup>/<sub>9</sub> code with noiseless feedback. Positional encoding and self-attention modules have no noticeable effect on BLER performance.

# B. Scaling laws: batch size

In section Section VII, we have demonstrated that it is possible to achieve performance comparable to GBAF with fewer parameters and lower compute complexity. We also hypothesized in Section VI-B that it is important to train the encoder using a very large batch size in order to accurately capture the statistics of the distribution so that the available power can be optimally allocated to the symbols

with error at the receiver while reducing the power to the remaining symbols in a batch. In deep learning literature, it is well known that increasing the batch size can noticeably improve the performance of the neural network model [29]. To better understand the effect of batch size on LIGHTCODE, we perform a systematic study by training LIGHTCODE with different batch sizes. As noted in Fig. 8, at a batch size of  $1.5 \times 10^3$ , LIGHTCODE has a BLER of  $3.7 \times 10^{-9}$ , similar to that of GBAF (w/o BU). However, the performance drops to  $4 \times 10^{-10}$ , exceeding GBAF, when the batch size increases to  $5 \times 10^4$  and beyond.

**Remark 1.** Using a lightweight network with a small number of parameters makes it feasible to train with very large batch size, resulting in a significantly lower error rate.

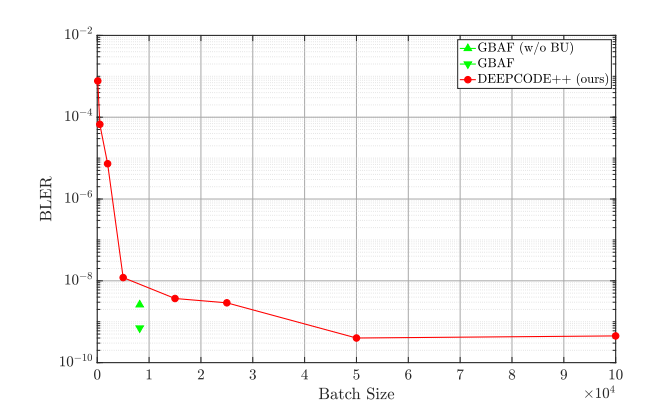


Fig. 8: BLER performance of LIGHTCODE with with respect to training batch size for rate  $^{3}/_{9}$  code at SNR -1.0 dB with noiseless feedback. Performance improves significantly with respect to batch size, surpassing the performance of GBAF at batch size  $> 5 \times 10^{4}$ .

#### C. Complexity and Throughput

Scheme	# parameters
GBAF [26]	$9.1 \times 10^{4}$
Robust Coding [24]	$8.6 \times 10^{4}$
LIGHTCODE (ours)	$7.3 imes 10^3$

TABLE IV: Rate  $^3/_9$  LIGHTCODE requires  $< ^1/_{10}$ <sup>th</sup> the number of parameters compared to GBAF and Robust Coding.

We compare the total number of parameters in the encoder and decoder for a rate  $^3/9$  LIGHTCODE against GBAF and Robust Coding within Table IV. LIGHTCODE reduces the parameter count by more than  $10\times$  compared to GBAF and Robust Coding, resulting in significant savings in memory.

To compare the throughputs, we measure the inference time in CPU mode on a AMD Ryzen Threadripper PRO 5975WX 32-Cores processor as well as in GPU mode using an NVIDIA GeForce RTX 4090, using a batch size of  $10^5-10^7$ . LIGHTCODE provides up to  $10\times$  higher throughput compared to GBAF. Further, LIGHTCODE provides up to  $171\times$  higher decoding throughput in CPU mode and up to  $10\times$  higher throughput in GPU mode compared to Robust Coding, providing significant gains in latency, as shown in Table V.

Scheme	Enc (CPU)	Dec (CPU)	Enc (GPU)	Dec (GPU)
GBAF [26]	$1.6 \times 10^{5}$	$1.7 \times 10^{6}$	$4.4 \times 10^{8}$	$3.3 \times 10^{9}$
Robust Coding [24]	$2.0 \times 10^{5}$	$7.6 \times 10^{4}$	$4.1 \times 10^{8}$	$2.4 \times 10^{9}$
LIGHTCODE (ours)	$1.5  imes 10^6$	$\boldsymbol{1.3\times10^7}$	$\boldsymbol{2.9\times10^9}$	$3.1\times10^{10}$

TABLE V: Throughput (symbols/sec) comparison. Rate  $^3/9$  LIGHTCODE achieves up to  $10\times$  higher decoding throughput compared to GBAF and up to  $171\times$  higher decoding throughput in CPU mode compared to Robust Coding.

# D. Interpretation of LIGHTCODE

By limiting to a symbol-by-symbol strategy, LIGHTCODE allows for better interpretability and analysis of the learned encoder representations compared to block coding schemes such as GBAF. By analyzing the power allocation and relation between encoder output and feedback from previous rounds, we draw connections between LIGHTCODE and POWERBLAST.

1) Power distribution: A key contributing factor to the superior performance of POWERBLAST compared to SK is the discrete-symbol scheme in the final round of communication. In the high-SNR regime, we are only interested in the error in the PAM index of the decoded symbol with respect to the original symbol; this will result in a sparse distribution where most of the samples are 0. Thus, a majority of the available power is naturally allocated to the symbol locations with non-zero error. Surprisingly, we find similar behavior for LIGHTCODE towards the final rounds of communication where the error is sparse.

To test this hypothesis, we choose a moderately sparse error regime for ease of analysis. In Fig. 9, we plot the power distribution of the encoder output in round 7 for rate  $^3/_9$  code at SNR -1.0 dB and noiseless feedback by randomly sampling 50 symbols. On the X-axis, we see the sample number, and on the Y-axis, we plot the magnitude of error in the integer PAM index of the estimate after round 6 and compare it against the magnitude of encoder output in round 7. Note that a difference in index of 1 corresponds to a magnitude of 2 in the unnormalized PAM from Eqn. III-A. It is evident from Fig. 9 that the highest power is allocated to the symbols with error in the estimate.

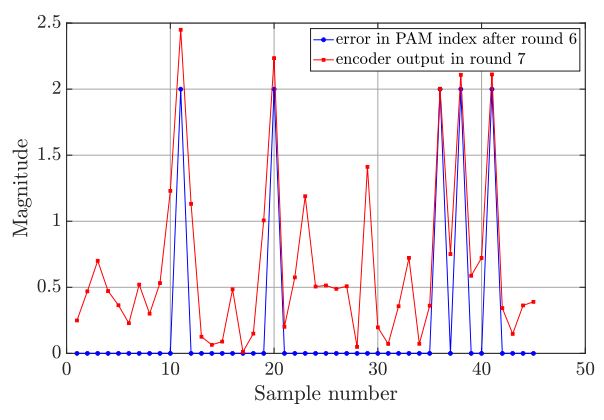


Fig. 9: LIGHTCODE allocates more power to the symbols with error in estimate from the previous round, improving the overall probability of decoding.

2) Interpreting the encoder: In Fig. 10, we plot the output of the encoder in round 2 with respect to the feedback in round 1. The encoder is approximately transmitting a linearly scaled

version of noise from round 1. Interestingly, for the symbols on the boundary of the constellation embeddings, the encoder does not need to transmit any data when the noise favors the ground truth, unlike in the SK scheme, where all noise needs to be corrected. For instance, consider  $\Theta_1$ , mapped to the symbol at the boundary on the left, where a negative noise in round 1 is favored. And  $\Theta_8$  is mapped to the symbol at the boundary on the right, where a positive noise in round 1 is favored. In such scenarios, the transmit power saved here can be reallocated to other symbols, improving the overall decoding error, which is only possible because of the non-linear activation functions.

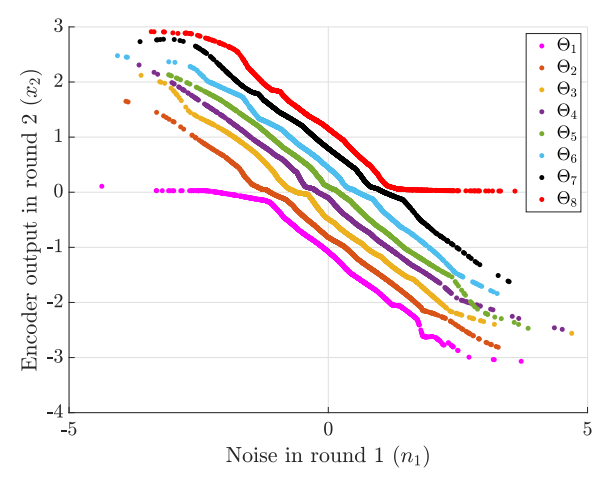


Fig. 10: Output of encoder in round 2  $(x_2)$  shows that the encoder is directly compensating for the noise experienced in round 1  $(n_1)$ .

Visualization of the encoder output beyond round 2 is difficult as the number of inputs to the encoder increases linearly with the number of rounds of communication. Alternatively, we test the linear dependency between  $x_{i+1}$  and  $\{x_1, \ldots, x_i, n_1, \ldots, n_i\}$  by performing a linear regression as

$$\hat{x}_{i+1} = \sum_{j=1}^{i} \alpha_j x_j + \beta_j n_j + c, \tag{20}$$

where  $\alpha_j$  and  $\beta_j$  are regression coefficients and c is the intercept found using LinearRegression toolbox in sklearn over  $10^6$  samples. To make the analysis tractable, we build one linear regression model for each symbol in the PAM constellation. In Fig. 11, we plot the predicted output using linear regression vs. true encoder output when the input PAM symbol index is  $\Theta=1$ , for rounds j=2 to 9. It is evident that as the round number increases, the relation becomes highly non-linear, and hence, classical schemes such as SK and GN as other linear schemes [6], [7] fail to model these dependencies.

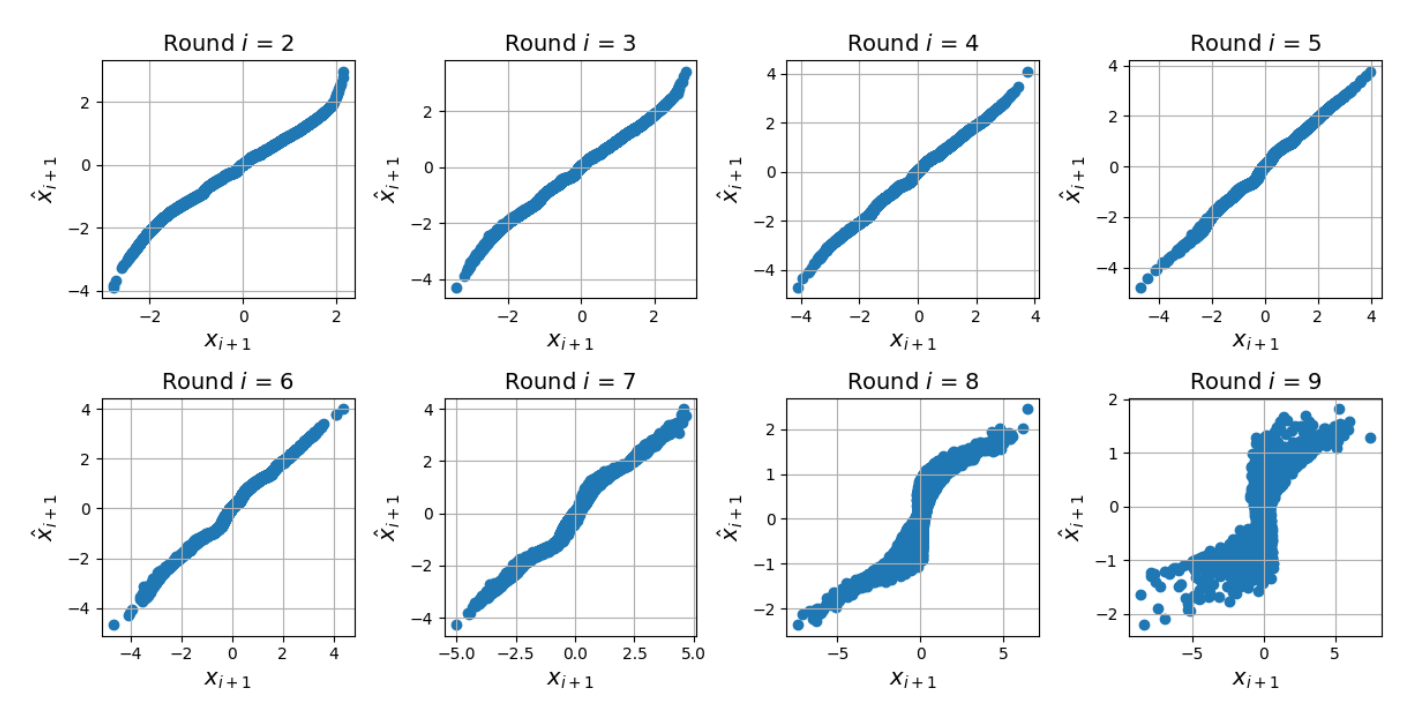


Fig. 11: Comparison of linear approximation (Y-axis) vs true encoder output (X-axis). As the rounds progress, the linearity of the relation between encoder output and the feedback from previous rounds breaks, making it harder for analytical schemes to perform well.

## IX. CONCLUSION

In this work, we address the problem of designing lightweight coding schemes for channels with feedback. First, we propose an analytical scheme, POWERBLAST, that can be viewed as a combination of Schalkwijk-Kailath and Gallager-Nakiböglu schemes. Using a hybrid strategy and taking advantage of the discrete nature of the signal in the final round, POWERBLAST noticeably outperforms both SK and GN, providing a performance that competes with current deep learning schemes in regions of high-SNR.

Next, we propose a lightweight deep-learning-based scheme, LIGHTCODE, that can achieve state-of-the-art BLER performance while using less than  $^1/10^{th}$  the parameters and compute complexity compared to existing deep-learning-based schemes. By limiting to a symbol-by-symbol strategy and carefully designing the feature extractor using skip connections, combined with a training strategy that uses a very large batch size of  $10^5$ , LIGHTCODE achieves a BLER up to  $\sim 10^{-10}$ .

Additionally, with the help of systematic ablation studies, we have demonstrated that the self-attention module in the transformer-based GBAF code has very little effect on the BLER performance, demonstrating the limited benefit of block coding in this regime.

Further, we interpret the LIGHTCODE to show that power distribution in the sparse error regime of LIGHTCODE is similar to that of POWERBLAST, where a majority of the available power is allocated to the symbols with error. Finally, we also perform a linear regression on the encoder outputs and the feedback from previous rounds. Our findings show that although the early stages of communication exhibit a linear relationship, it becomes non-linear towards the later stages, underscoring the importance of employing deep-learning-based

non-linear coding techniques to attain optimal performance in regions of extremely low SNR.

#### REFERENCES

- [1] C. Shannon, "The zero error capacity of a noisy channel," *IRE Transactions on Information Theory*, vol. 2, no. 3, pp. 8–19, 1956.
- [2] J. Schalkwijk and T. Kailath, "A coding scheme for additive noise channels with feedback-i: No bandwidth constraint," *IEEE Transactions* on *Information Theory*, vol. 12, no. 2, pp. 172–182, 1966.
- [3] J. Schalkwijk, "A coding scheme for additive noise channels with feedback-ii: Band-limited signals," *IEEE Transactions on Information Theory*, vol. 12, no. 2, pp. 183–189, 1966.
- [4] R. G. Gallager and B. Nakiboğlu, "Variations on a theme by schalkwijk and kailath," *IEEE Transactions on Information Theory*, vol. 56, no. 1, pp. 6–17, 2009.
- [5] A. Ben-Yishai and O. Shayevitz, "Interactive schemes for the awgn channel with noisy feedback," *IEEE Transactions on Information Theory*, vol. 63, no. 4, pp. 2409–2427, 2017.
- [6] Z. Chance and D. J. Love, "Concatenated coding for the awgn channel with noisy feedback," *IEEE Transactions on Information Theory*, vol. 57, no. 10, pp. 6633–6649, 2011.
- [7] R. Mishra, D. Vasal, and H. Kim, "Linear coding for awgn channels with noisy output feedback via dynamic programming," *IEEE Transactions* on *Information Theory*, 2023.
- [8] J. M. Ooi and G. W. Wornell, "Fast iterative coding techniques for feedback channels," *IEEE Transactions on Information Theory*, vol. 44, no. 7, pp. 2960–2976, 1998.
- [9] A. G. Perotti, B. M. Popovic, and A. R. Safavi, "Accumulative iterative codes based on feedback," arXiv preprint arXiv:2106.07415, 2021.
- [10] S. K. Ankireddy, S. A. Hebbar, Y. Jiang, P. Viswanath, and H. Kim, "Compressed error harq: Feedback communication on noise-asymmetric channels," in 2023 IEEE International Symposium on Information Theory (ISIT). IEEE, 2023, pp. 1160–1165.
- [11] J. Griffin, P. Yuan, P. Popovski, K. R. Duffy, and M. Médard, "Code at the receiver, decode at the sender: Grand with feedback," in 2023 IEEE Information Theory Workshop (ITW). IEEE, 2023, pp. 341–346.
- [12] M. Raghu, B. Poole, J. Kleinberg, S. Ganguli, and J. Sohl-Dickstein, "On the expressive power of deep neural networks," in *international conference on machine learning*. PMLR, 2017, pp. 2847–2854.
- [13] E. Nachmani, Y. Be'ery, and D. Burshtein, "Learning to decode linear codes using deep learning," in 2016 54th Annual Allerton Conference on Communication, Control, and Computing (Allerton). IEEE, 2016, pp. 341–346.

- [14] E. Nachmani, E. Marciano, L. Lugosch, W. J. Gross, D. Burshtein, and Y. Be'ery, "Deep learning methods for improved decoding of linear codes," IEEE Journal of Selected Topics in Signal Processing, vol. 12, no. 1, pp. 119-131, 2018.
- [15] S. K. Ankireddy and H. Kim, "Interpreting neural min-sum decoders," in ICC 2023-IEEE International Conference on Communications. IEEE, 2023, pp. 6645-6651.
- [16] S. A. Hebbar, R. K. Mishra, S. K. Ankireddy, A. V. Makkuva, H. Kim, and P. Viswanath, "Tinyturbo: Efficient turbo decoders on edge," in 2022 IEEE International Symposium on Information Theory (ISIT). IEEE, 2022, pp. 2797-2802.
- [17] S. A. Hebbar, V. V. Nadkarni, A. V. Makkuva, S. Bhat, S. Oh, and P. Viswanath, "Crisp: Curriculum based sequential neural decoders for polar code family," in International Conference on Machine Learning. PMLR, 2023, pp. 12823-12845.
- [18] S. A. Hebbar, S. K. Ankireddy, H. Kim, S. Oh, and P. Viswanath, "Deeppolar: Inventing nonlinear large-kernel polar codes via deep learning, arXiv preprint arXiv:2402.08864, 2024.
- [19] Y. Li, Z. Chen, G. Liu, Y.-C. Wu, and K.-K. Wong, "Learning to construct nested polar codes: An attention-based set-to-element model,' IEEE Communications Letters, vol. 25, no. 12, pp. 3898–3902, 2021.
- [20] S. K. Ankireddy, S. A. Hebbar, H. Wan, J. Cho, and C. Zhang, "Nested construction of polar codes via transformers," arXiv preprint arXiv:2401.17188, 2024.
- [21] H. Kim, Y. Jiang, S. Kannan, S. Oh, and P. Viswanath, "Deepcode: Feedback codes via deep learning," Advances in neural information processing systems, vol. 31, 2018.
- [22] A. R. Safavi, A. G. Perotti, B. M. Popovic, M. B. Mashhadi, and D. Gunduz, "Deep extended feedback codes," arXiv preprint arXiv:2105.01365,
- [23] M. B. Mashhadi, D. Gunduz, A. Perotti, and B. Popovic, "Drf codes: Deep snr-robust feedback codes," arXiv preprint arXiv:2112.11789,
- [24] J. Kim, T. Kim, D. Love, and C. Brinton, "Robust non-linear feedback coding via power-constrained deep learning," arXiv preprint arXiv:2304.13178, 2023.
- [25] Y. Shao, E. Ozfatura, A. Perotti, B. Popovic, and D. Gündüz, "Attentioncode: Ultra-reliable feedback codes for short-packet communications," IEEE Transactions on Communications, 2023.
- [26] E. Ozfatura, Y. Shao, A. G. Perotti, B. M. Popović, and D. Gündüz, "All vou need is feedback: Communication with block attention feedback codes," IEEE Journal on Selected Areas in Information Theory, vol. 3, no. 3, pp. 587-602, 2022.
- [27] P. Elias, "Channel capacity without coding," in Lectures on Communication System Theory, E. Baghdady, Ed. New York: McGraw Hill, 1961, quarterly progress report, MIT Research Laboratory of Electronics, Oct
- [28] M. Agrawal, D. J. Love, and V. Balakrishnan, "An iteratively optimized linear coding scheme for correlated gaussian channels with noisy feedback," in 2011 49th Annual Allerton Conference on Communication, Control, and Computing (Allerton). IEEE, 2011, pp. 1012–1018.
- [29] Y. Bahri, E. Dyer, J. Kaplan, J. Lee, and U. Sharma, "Explaining neural scaling laws," arXiv preprint arXiv:2102.06701, 2021.

# APPENDIX A ALGORITHM FOR GALLAGER-NAKIBÖGLU

# Algorithm 4: Gallager-Nakibŏglu coding scheme

**Input:** Message symbol  $\Theta$ , number of rounds D, noise variance  $\sigma_{ff}^2$ 

**Round 1: Tx:** Power normalization:  $X_1 = \sqrt{P_1}\Theta$ ;

Transmit:  $Y_1 = X_1 + N_1$ ;

**Rx:** Send  $Y_1$  as feedback to Tx;

/\* Tx sends the noise  $U_2=N_1$  in round

**Round 2: Tx:** Power normalization:  $X_2 = \frac{\sqrt{P_2}U_2}{\sigma_2}$ ; where  $U_2 = N_1$  and  $\sigma_2 = \sigma_{ff}$ ;

Transmit:  $Y_2 = X_2 + N_2$ ;

Rx: Compute the LMMSE estimate of transmit symbol  $\mathbb{E}[U_2|Y_2] = \frac{\sigma_2\sqrt{P_2}Y_2}{1+P_2};$ 

Update the estimate as  $\hat{X}_1 = X_1 - \mathbb{E}[U_2|Y_2]$ 

/\* Tx sends the error in estimate  $\epsilon_2 = \mathbb{E}[U_2|Y_2] - U_2$  over the next D-2rounds \*/

while  $3 \le i \le D - 1$  do

**Tx:** Compute the error in estimate of previous round  $U_i = \mathbb{E}[U_{i-1}|Y_{i-1}] - U_{i-1}$ ;

Power normalization:  $X_i = \frac{\sqrt{P_2}U_i}{\sigma_i}$ , where  $\sigma_i^2 = \frac{\sigma_{i-1}^2}{1+S_{i-1}}$ ; Transmit:  $Y_i = X_i + N_i$ ;

**Rx:** Send feedback as LMMSE estimate of transmit symbol  $\mathbb{E}[U_i|Y_i] = \frac{\sigma_i\sqrt{P_2}Y_i}{1+P_2}$ ;

Update the estimate as  $\hat{X}_1 = X_1 - \sum_{j=2}^{j=i} \mathbb{E}[U_j|Y_j]$ 

**Decoding after round** D-1: Map  $\hat{\Theta}_{D-1} = \frac{\hat{X_1}}{\sqrt{P_1}\eta}$  to the closest symbol in the  $2^K$  PAM constellation.

 $/\star$  High-SNR scheme for rounds D  $\star/$ 

Round D: Tx: Compute the difference in PAM indices  $U_D = \hat{m} - m$ ;

Power normalization:  $X_D = \frac{\sqrt{P_2}U_D}{\sigma_D}$ ; where  $U_D = \hat{m} - m$  and  $\sigma_D = \sigma_{ff}$ ; Transmit:  $Y_D = X_D + N_D$ ;

**Final Decoding**: Use ML decoder to detect  $\hat{U}$  and detect original PAM signal using  $\hat{U}$ .